

Sporadic meteor radiant distributions: orbital survey results

J. Jones and P. Brown

Department of Physics, University of Western Ontario, London, Ontario N6A 3K7, Canada

Accepted 1993 May 14. Received 1993 May 13; in original form 1993 March 9

ABSTRACT

The structure of the sporadic meteor complex is determined from the data in 10 orbital surveys. In addition to the previously known apex, helion, antihelion and northern toroidal sources, we find a southern toroidal source and a splitting of the apex source. The size of the sources and possible origin of meteoroids from each region are discussed.

Key words: meteoroids.

1 INTRODUCTION

Throughout the history of meteor astronomy, scientists have been preoccupied with the study of meteor showers to the virtual exclusion of other aspects of the meteoric background. This concept of a meteoric ‘background’ became important primarily in relation to meteor showers, and was usually regarded as something to be filtered out of the shower activity where the real information lay. Indeed, some of the earliest work on sporadic meteor radiant distributions was carried out on the assumption that most or all meteors belonged to streams – the majority much weaker than the familiar regular streams of today. For the purposes of this paper, we choose to define a sporadic meteor as one that does not belong to one of the major showers. We use this definition for pragmatic reasons, and do not wish to imply that sporadic meteors have any special origin or history.

The earliest concepts about sporadic meteors appear to have originated with Schiaparelli (1866). He theorized that radiants of uniform intensity were also uniformly distributed in the sky, with the meteors moving at the parabolic limit. As a result, the only concentration would be due to the Earth’s orbital motion in the direction of the apex. This model yielded only very limited agreement with observations. In 1878, von Niessl attempted to improve the fit with observations by assuming hyperbolic velocities, but with little success.

The first serious observational work on sporadic meteors was published by Denning (1866, 1899), who also summarized the work of most of his contemporaries and analysed the distribution of radiants over the sky. On the incorrect assumption that meteors occurring at widely different times are associated with the same radiant, he identified many meteor streams, most of which are probably spurious. He found some indication of an excess of shower radiants west of the Earth’s apex, and proposed that the Earth actually encounters regions of increased meteoroid density at certain

times of the year; he also noted the marked seasonal variation in meteor rates between summer and winter.

In spite of Denning’s work, the idea that meteor radiants were essentially randomly distributed in the sky, and that the only concentration of the sporadic meteor component came from the apex, became firmly entrenched for the next half-century. Although the overriding question of the time was whether there was a significant hyperbolic component among sporadic meteors, several major observational efforts were undertaken to determine diurnal and seasonal rate variations. Notable among these was the extensive effort of Hoffmeister (1948), who found a strong ecliptical component to the sporadic background. This picture of the sporadic radiant distribution remained firmly intact into the mid-1950s, as demonstrated by visual studies, such as those of Murakami (1956), who found the heliocentric distribution of sporadic meteor radiants to be quite uniform.

Hawkins (1956b) published the results of observations with the Jodrell Bank meteor-radar system and revised the picture of sporadic distributions. He found that sporadic radiants were concentrated in the ecliptic plane in three principal sources: an apex source, an antihelion component and a helion source. This picture was supported by visual observations showing strong antihelion and apex sporadic sources (Hawkins & Prentice 1957). Hawkins’ work still forms the basis for almost all work done on sporadic distributions. Extensive discussion of the nature of these sources can be found in the work of Davies (1957).

Hawkins’ model, which used observations from the northern hemisphere, was extended by Weiss & Smith (1960), who employed radio-meteor data gathered in Australia. They confirmed Hawkins’ picture, detecting three principal sporadic sources at the apex, antihelion and helion points. Keay (1963) found that this three-source picture adequately explained the diurnal rate variations detected by the radar system in Adelaide, and suggested that their relative strengths were 2:1:2 for the helion, apex and antihelion

Table 1. Details of surveys employed for sporadic distributions (see Lindblad 1992).

Name	Type of Survey	No. of Meteor Orbits	Less Six Showers	Less Twenty Showers	Year
Harvard I	Radar	19327	17838	15186	1961-1965
Harvard II	Radar	19698	18853	16269	1968-1969
Adelaide I	Radar	2092	1774	1336	1960-1961
Adelaide II	Radar	1667	1527	1335	1968-1969
Obninsk	Radar	9354	8000	7215	1967-1968
Kharkov	Radar	5327	5093	4560	1975
Super-Schmidt	Photo	2529	2213	1679	1952-1954
Soviet Photo	Photo	1111	622	419	1952-1976
Harvard Precise	Photo	1245	1015	712	1936-1959
Fireball	Photo	554	512	354	1963-1983

sources respectively. Moreover, he noted that the strength of the sources seemed to vary widely during the year, confirming the earlier conclusions of Davies & Gill (1960) from a study of faint sporadic meteor orbits.

Stohl (1968), after analysing data from the Springhill Meteor Radar in Canada, extended the model to include a fourth source, which he called the 'toroidal source', located at ecliptic latitude $+60^\circ$, with the same Sun-centred longitude as the apex source.

This basic four-source picture has persisted to the present, although many still use the simple three-source model of Hawkins. Not only is it an interesting astronomical problem to explain the observed radiant distribution, but it is also important to describe the sporadic radiant distribution accurately to obtain reliable predictions of the performance of forward-scatter meteor burst communication systems (Meeks & James 1959; Weitzen 1986).

Both Davies' (1957) and Hawkins' (1956) studies use data from one of the earliest meteor radars at Jodrell Bank. Since then, there have been numerous large radar surveys, including the Harvard Radio Survey (Sekanina 1976), and additional photographic data such as those of McCrosky & Posen (1961). The raw data from all these surveys have recently become available through the IAU Meteor Data Center in Lund, Sweden (Lindblad 1987). The present work uses data from the IAUMDC to determine the significant sporadic sources on the celestial sphere, including their sizes, locations and orbital distributions; the overall purpose is to bring the pioneering work of Hawkins up to date, and to re-evaluate the spatial distribution of sporadic meteors.

2 THE OBSERVATIONS

10 surveys were selected from the IAUMDC to study the sporadic complex. Details of each survey are presented in Table 1. The orbital data from the surveys were used to filter out major meteor showers which might interfere with the sporadic background, particularly for the relatively small photographic surveys. To do this, the stream elements for the showers listed in Table 2 were used, and each orbit in all the surveys was compared with these mean stream orbits. The shower members were removed on the basis of Hawkins &

Table 2. Meteor streams and their associated orbital elements filtered out of the surveys. Here ω is the argument of perihelion in degrees, e is the orbital eccentricity, q is the perihelion distance in au, i is the inclination, and Ω is the longitude of the ascending node (1950.0). From McKinley (1961) and Cook (1973).

Stream	ω	e	q	i	Ω
Perseids	151.5	0.965	0.953	113.8	139
Geminids	324.3	0.896	0.142	23.6	261
Orionids	82.5	0.962	0.571	163.9	28
Arietids	29	0.94	0.09	21	77
Quadrantids	170	0.683	0.977	72.5	282.7
Delta Aquarids	152.8	0.976	0.069	27.2	305
Zeta Perseids	60	0.79	0.35	0	78
North Delta Aquarids	333	0.973	0.07	20	139
South Iota Aquarids	128	0.92	0.23	6	311
North Iota Aquarids	308	0.84	0.27	5	151
Kappa Cygnids	204	0.76	0.97	37	144
Lyrids	214	0.97	0.92	80	32
Eta Aquarids	109	0.83	0.70	158	44
Beta Taurids	246	0.85	0.34	6	276
South Taurids	112	0.84	0.37	5	45
North Taurids	298	0.85	0.32	3	222
Alpha Capricornids	271	0.78	0.57	4	133
Giacobinids	172	0.72	0.996	30.7	196.2
Leonids	174	0.92	0.97	163	235
Ursids	212	0.85	0.92	53	265

Southworth's D criterion, which is a measure of orbital similarity such that identical orbits have a D coefficient of zero. We have found that a value of D of 0.5 is usually required to remove all the meteors associated with the major streams from the data; a lower value of D tends to leave a detectable residue of shower meteors. Table 1 lists the number of meteors remaining after the first six streams in Table 2 have been compared with the survey orbits, and the number that remain after all the showers in Table 2 have been compared to the surveys. The final distributions with 20 streams

removed do not differ significantly from those with only the first six removed; we therefore choose for this work to use the data with the six major streams removed. We note that, by increasing the number of showers to be filtered out or by increasing the acceptable value of the D criterion, we could have removed the sporadic background entirely, but in that case the radiant distribution could not be described simply. The meteor showers were most conspicuous in the Super-Schmidt data of McCrosky & Posen (1961), and Figs 1 and 2 show the effect of the six-stream sieve, which is similar to that of the 20-stream sieve, although, of course, the latter comprises fewer meteors. To define contours on these maps, the celestial sphere was broken up into $5^\circ \times 5^\circ$ squares, and meteors in each of these regions were counted. The relative radiant density in each area was then compared using contour plots.

3 RESULTS

The final distributions for some selected surveys are given in Figs 3–6, which are from the perspective of an observer looking towards the apex. The coordinates are expressed in terms of a Sun-centred longitude ($L = \lambda - \lambda_0$) and ecliptic latitude (β). Inspection of these activity profiles reveals immediately that there are several major sporadic sources common to these surveys. The antihelion (AH) activity source is prominent in all surveys, occurring close to Sun-centred longitude $\sim 190^\circ$ and ecliptic latitude 0° . The ‘partner’ source to this is the helion (H) source, visible in all the radar surveys (although it is not present in the photographic data which are necessarily gathered during the hours of darkness) at longitude $\sim 345^\circ$ and 0° ecliptic latitude. The other two clearly visible radar sources are the north toroidal (NT)

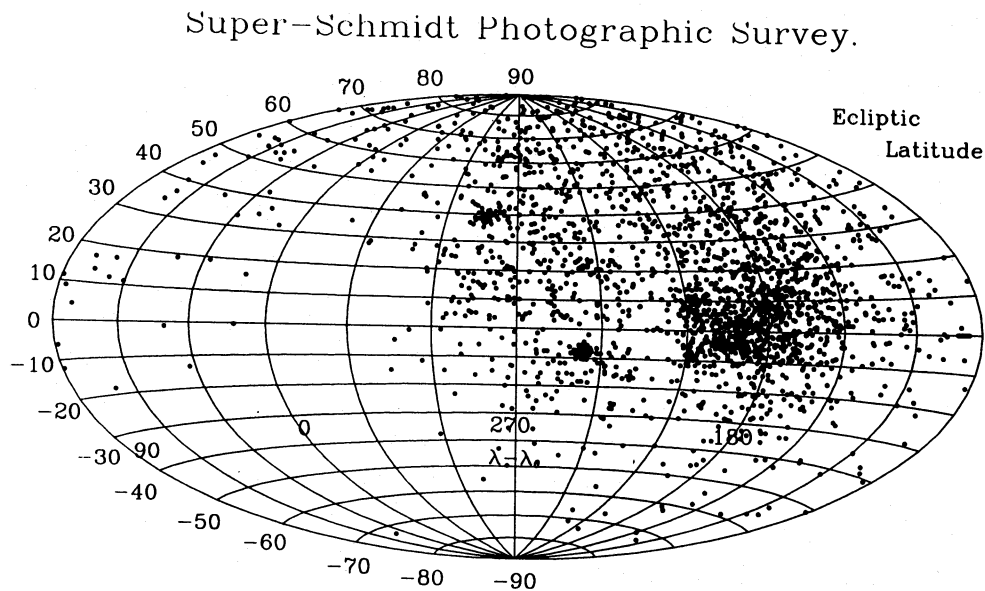


Figure 1. Individual radiant points for all meteors in the Super-Schmidt survey.

Super-Schmidt Photographic Survey (six showers removed).

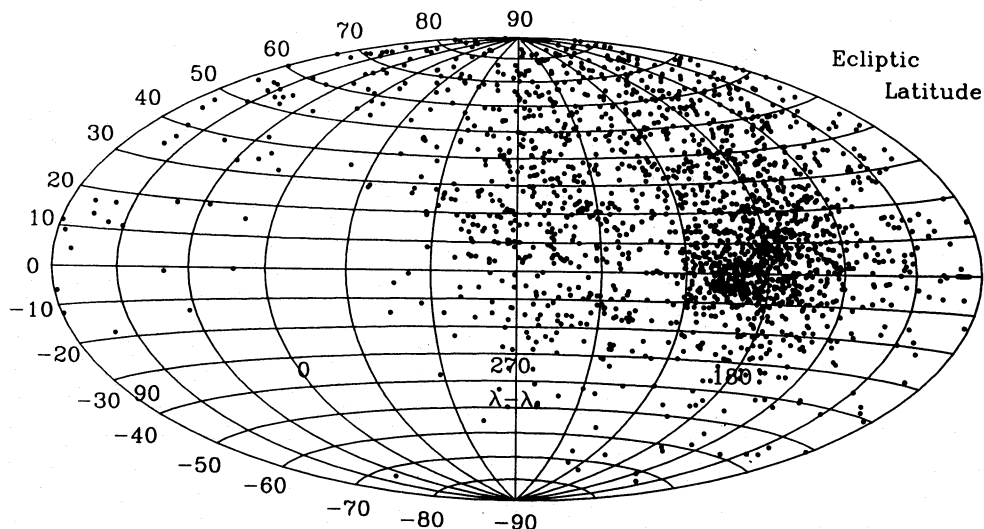


Figure 2. Individual radiant points for the meteors remaining in the Super-Schmidt survey after six showers have been removed.

Combined Harvard Radio Surveys

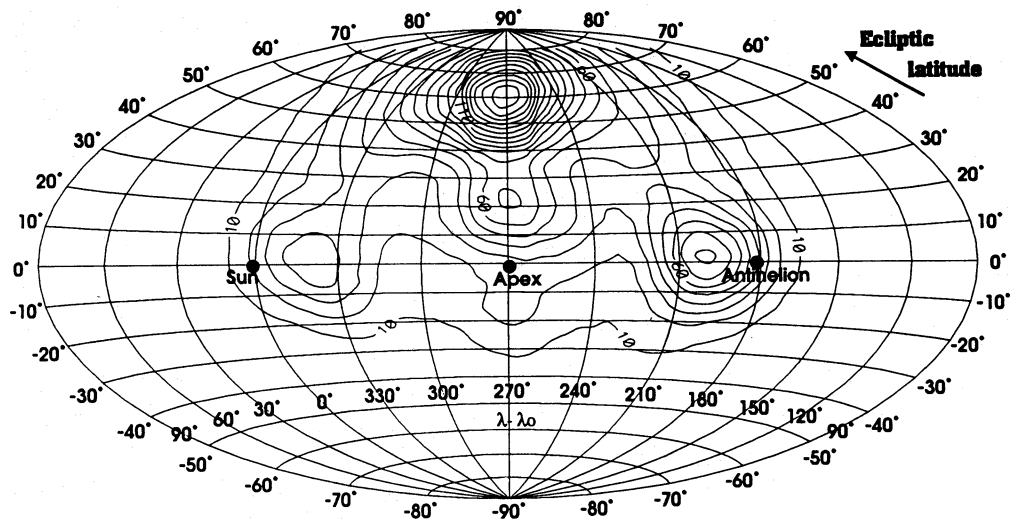


Figure 3. Activity contours for the combined Harvard radio surveys (a compilation of the Harvard I and Harvard II surveys). The abrupt ending of the contours near the edges of the projection is an artefact of the contour-smoothing method employed.

Combined Adelaide Radio Surveys

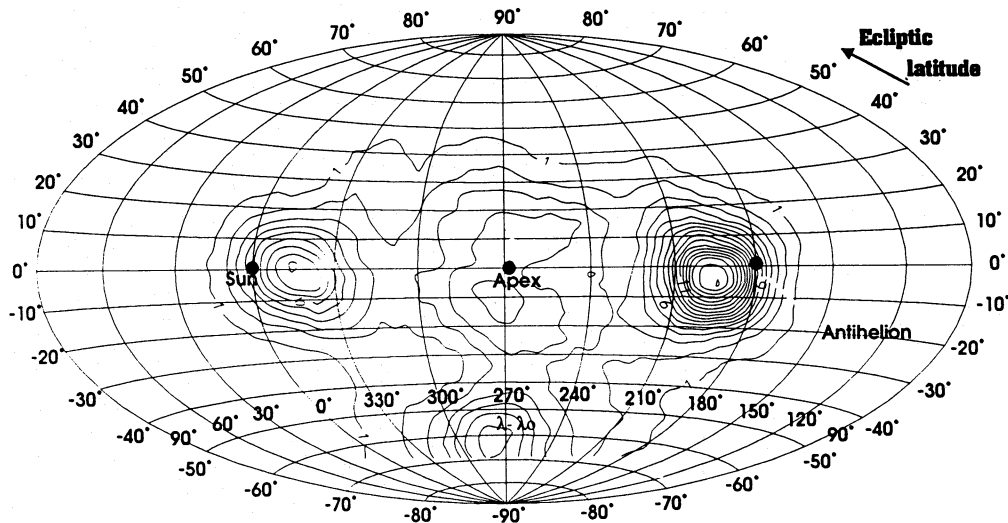


Figure 4. Activity contours for the combined Adelaide radio surveys (a compilation of the Adelaide I and Adelaide II surveys). See caption to Fig. 3 for details.

source located near 270° longitude and $+60^\circ$ latitude, and its partner source, the south toroidal (ST) component located near 270° longitude and -60° latitude. In addition, several northern radar surveys clearly show a ‘north’ apex (NA) source, at 270° longitude and $+20^\circ$ latitude, which is also weakly discernible on some photographic surveys. The partner source of this is the south apex (SA) source, which is weakly visible in some northern radar surveys and somewhat more clearly in the Adelaide work. Unfortunately, the Adelaide surveys were relatively small, and so the numbers involved leave the physical character of the SA source open to question.

For all the surveys, the centres of each of these sources, if visible, were measured and their widths at half-maximum in

all the cardinal directions determined in angular terms. In Table 3, the mean radius of each source and its position in each survey are given. In addition, the relative strength of each source, normalized to the strongest source within a given survey, is presented. Table 4 presents the mean characteristics for each source in the radar surveys. The photographic surveys contain so little data relative to the radar work that we omit them from the mean values.

The source strengths vary widely from survey to survey. In addition, the position and visibility of each sporadic source differ somewhat between surveys. This is probably the result of the lack of uniform corrections applied to all the data, such as a velocity correction in the case of radar data. Initial train radius is also a significant cause of bias in the estimate

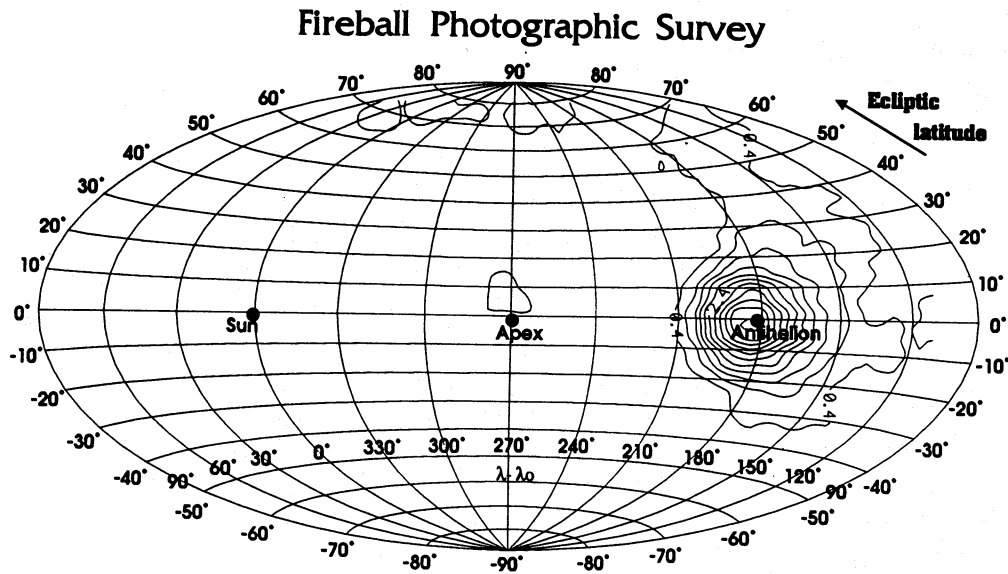


Figure 5. Activity contours for the fireball photographic survey. See caption to Fig. 3 for details.

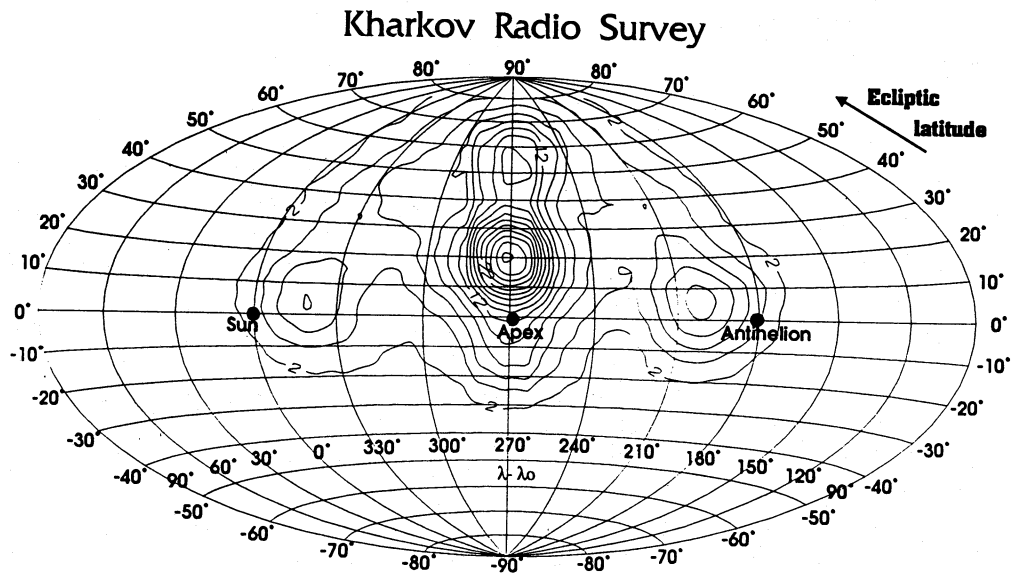


Figure 6. Activity contours for the Kharkov radio survey. See caption to Fig. 3 for details.

of the source strengths for the radar surveys, as are the particular antenna gain pattern and geometry for a given system. Angular velocity plays a strong role in detection for the photographic surveys. This may explain, in part, why the apex sources are in general rather weak compared with the other sources. It should be noted that, for unknown reasons, the Obninsk survey has all orbits with southern ecliptic latitude radiants removed before entry into the IAUMDC. All data used were exactly as given in the IAUMDC.

The widths of the sources vary for numerous selection reasons, and there is certainly an intrinsic mass dependence. For example, the photographic source widths appear smaller than the radar widths, as would be expected since the smaller radar particles will be influenced much more strongly by radiation forces than the larger photographic particles as a result of their larger surface-to-mass ratio.

In spite of the difference in the observational systems and locations, there is much agreement between the surveys. The placement of the source positions is roughly the same (within the 2° – 3° accuracy of the grid smoothing used), and the existence of six major sources is established.

4 DISCUSSION

The original three-source picture by Hawkins can be considered a first-order approximation to the present six-source model. The AH and H sources from his work are clearly represented here, and his apex source appears to be split into northern and southern branches.

To investigate the orbital element distribution of meteoroids from each of the sporadic sources, all meteoroid orbits from each survey with radiants within the mean width for a

Table 3. Characteristics of sporadic sources. Radii are in deg, longitude is Sun-centred, and latitude is ecliptic.

Survey	Data	AH	H	NA	SA	NT	ST
Harvard I	radii	25	20	23	-	23	-
	strength	.58	.35	.46	.18	1	-
	long	199	341	269	275	273	-
	lat	3	2	28	-11	59	-
Harvard II	radii	18	19	22	-	18	-
	strength	.37	.20	.35	.10	1	-
	long	199	341	270	270	274	-
	lat	2	2	25	-15	59	-
Adelaide I	radii	16	15	-	-	-	17
	strength	1	.57	.14	.24	-	.33
	long	193	345	273	272	-	267
	lat	-4	0	11	-15	-	-59
Adelaide II	radii	14	10	-	-	-	15
	strength	1	.44	.47	.44	-	.63
	long	195	344	272	273	-	280
	lat	-5	0	7	-6	-	-60
Obninsk	radii	-	-	23	-	-	-
	strength	-	-	268	-	-	-
	long-lat	-	-	20	-	-	-
Kharkov	radii	17	16	15	-	17	-
	strength	.33	.27	1	-	.53	-
	long	201	341	272	-	267	-
	lat	5	3	20	-	55	-
SuperSchmidt	radii	17	-	-	-	-	-
	strength	189	-	-	-	-	-
	long-lat	3	-	-	-	-	-
Sov.Photo	radii	19	-	-	-	-	-
	strength	187	-	-	-	-	-
	long-lat	3	-	-	-	-	-
Harv.Precise	radii	13	-	-	-	-	-
	strength	189	-	-	-	-	-
	long-lat	3	-	-	-	-	-
Fireball	radii	15	-	8	-	-	-
	strength	1	-	.14	-	-	-
	long-lat	184	-	273	-	-	-

Table 4. Mean source characteristics.

Source	AH	H	NT	ST	NA	SA
Position	198,0	342,1	271,58	274,-60	271,19	273,-11
Radii	18	16	19	16	21	-

particular survey were selected. The cumulative distribution for each source region was then found, based on data from all 10 surveys. The results are presented in Figs 7–9, which are based predominantly on radar meteor data and therefore best reflect the small-particle population.

From an examination of these graphs, several points become immediately clear. The H and AH sources are populated by low-inclination, prograde eccentric orbits which are essentially identical to short-period comets and may also have an asteroidal component. The velocity distribution provides the low-tail end of the overall geocentric velocity curve peaking near 31 km s^{-1} . We note that from other work (Keay

1963; Stohl 1968) it is generally agreed that the AH source is the stronger of the two. This is puzzling, as the two sources sample essentially the same particle population and hence should have the same strength; perhaps the different strengths are attributable to a day–night effect in the atmosphere rather than a true intrinsic difference.

For the NA source, the situation is quite different. Here some highly eccentric orbits are present, but more circular orbits tend to dominate. We see a preponderance of high-inclination (retrograde) orbits as well as local maxima just under $i = 90^\circ$. The latter are particles the Earth catches up to, while the former are head-on collisions. The velocity distribution also shows this double-hump effect, though the average is near 53 km s^{-1} , attesting to the dominance of retrograde particles from the NA source. The NA source is most evident in the radar surveys, suggesting that smaller particles are the principal component. The orbital elements of these particles are very similar to those of the long-period comets. From arguments of symmetry, the SA source would probably have the same general particle population.

The NT source is the most intriguing. The absence of the toroidal sources from Hawkins' work can be attributed to relatively insensitive radar and small numbers of meteors. In fact, Davies (1957), having investigated a small number of orbits (~ 2000) for sporadic meteors from another radar system at Jodrell Bank, did detect the NT source, and suggested that it was caused by small particles moving in near-circular orbits. He even proposed that these small, high-inclination particles could have originated in long-period orbits that have now circularized under the influence of Poynting–Robertson drag. His orbital distribution showed a clear peak near $i = 60^\circ$ and 140° for this class of particles. Davies & Gill (1960) came to the same conclusions. It is difficult to conceive of a non-cometary origin for such high-inclination particles. The present work shows the toroidal population to be composed of relatively circular orbits with a clear, Gaussian distribution of inclinations about the mean of $i = 60^\circ$. We also note that the radar data for which the NT source is most visible have all been derived from three-station radars which rely on measurements of the Fresnel zones to derive accurate orbits. Fragmentation tends to smear the Fresnel pattern in the echoes, so there is a possibility that fragmenting meteoroids are underrepresented in these surveys. Recently, Baggaley, Steel & Taylor (1992) have developed a radar that allows meteor orbits to be measured independently of the Fresnel oscillations, and it would be interesting to see whether the toroidal sources are still prominent when measured in this way. Thus the radar data have a heavy bias toward compact, non-fragmenting meteors, and this may be one of the systematic effects that modify the source characteristics from one radar system to the next. Additionally, the atmosphere is a strong source of bias in radar observations (cf. Lindblad 1968).

Little has been said in the literature about the origin of these small, highly inclined particles. It is possible that much of the strength previously attributed to apex particle concentrations in radio work is actually due to the toroidal source. The distribution about $i = 60^\circ$ might lead to speculation that all these particles have a single origin: perhaps a large, long-period comet deposited this material long ago, and the orbits for the smaller particles have now circularized under Poynting–Robertson drag, as Davies originally

North Apex Source

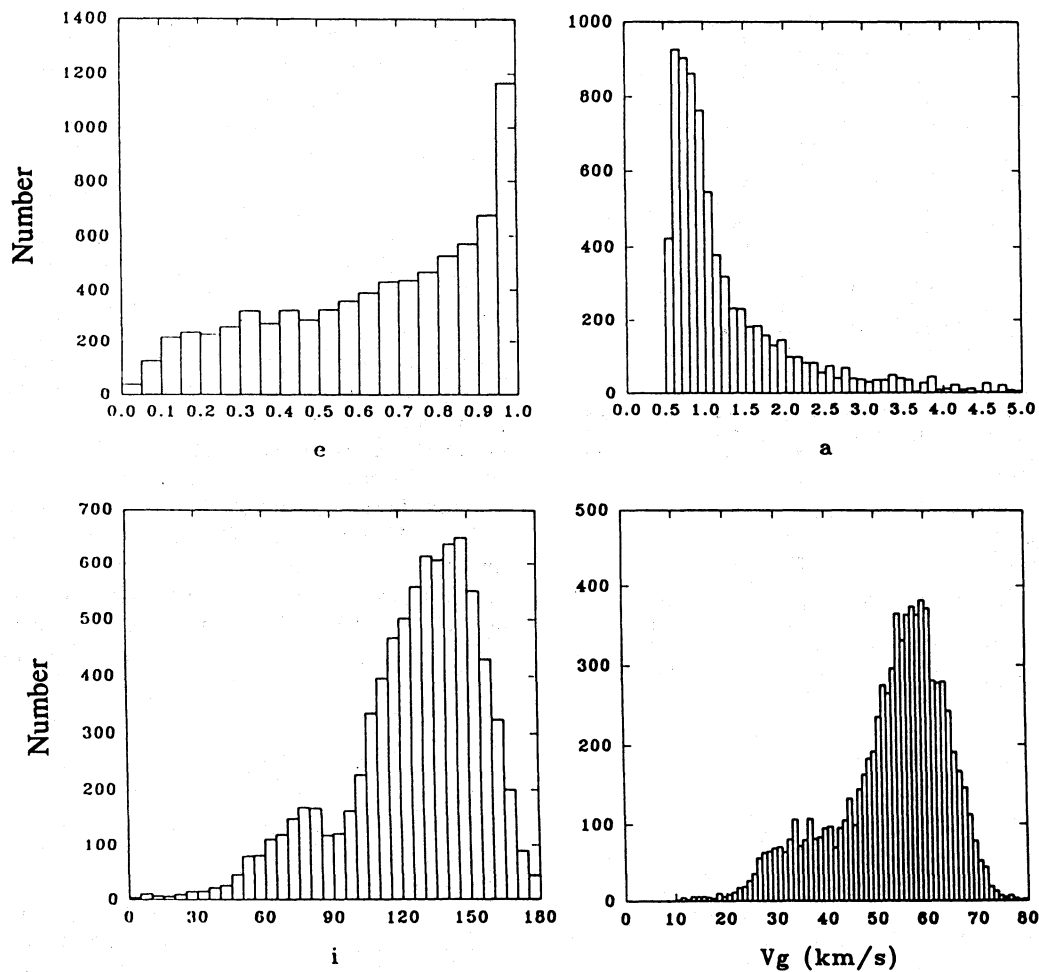


Figure 7. The orbital elements for the north apex source region. The plots represent (clockwise from upper left) the eccentricity (e) distribution, the distribution of the semimajor axis (a) in au, the geocentric velocity V_g in km s^{-1} and the inclination i in deg.

Antihelion Source

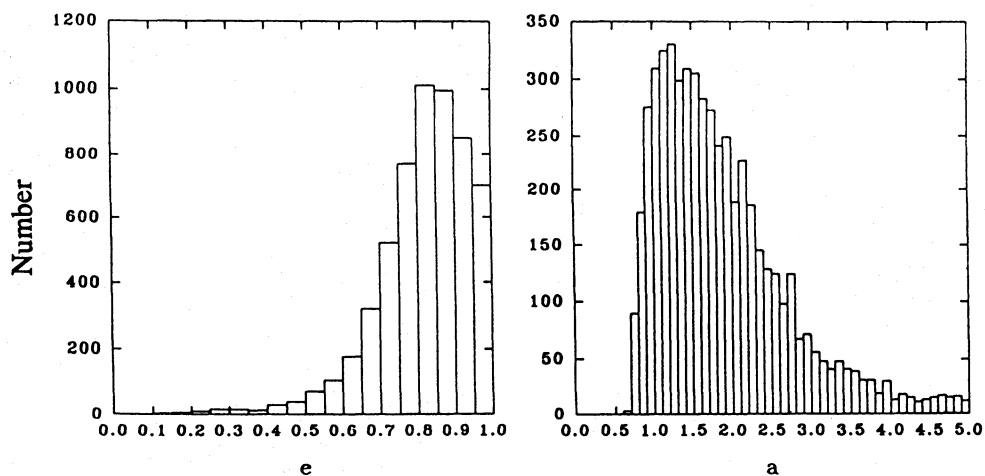


Figure 8. The orbital elements for the antihelion source region. Details as in caption to Fig. 7.

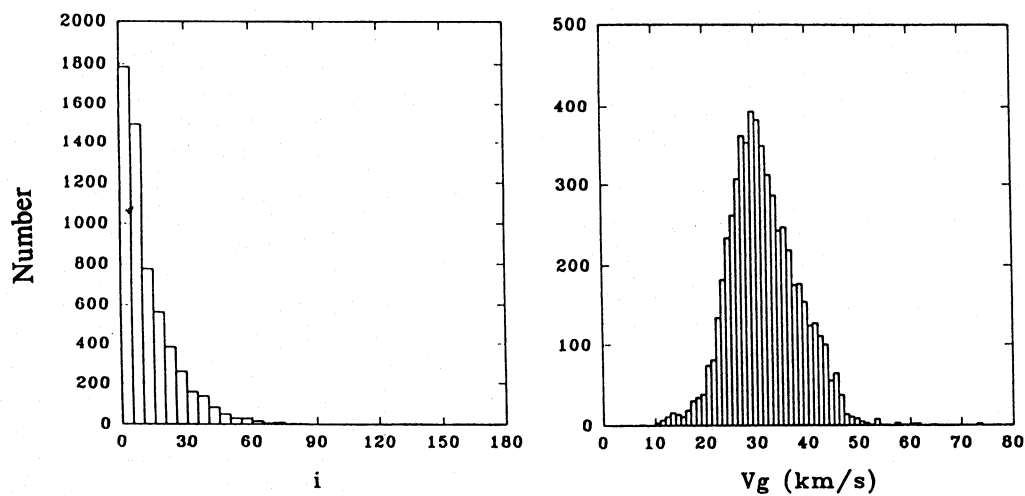


Figure 8 - continued

North Toroidal Source

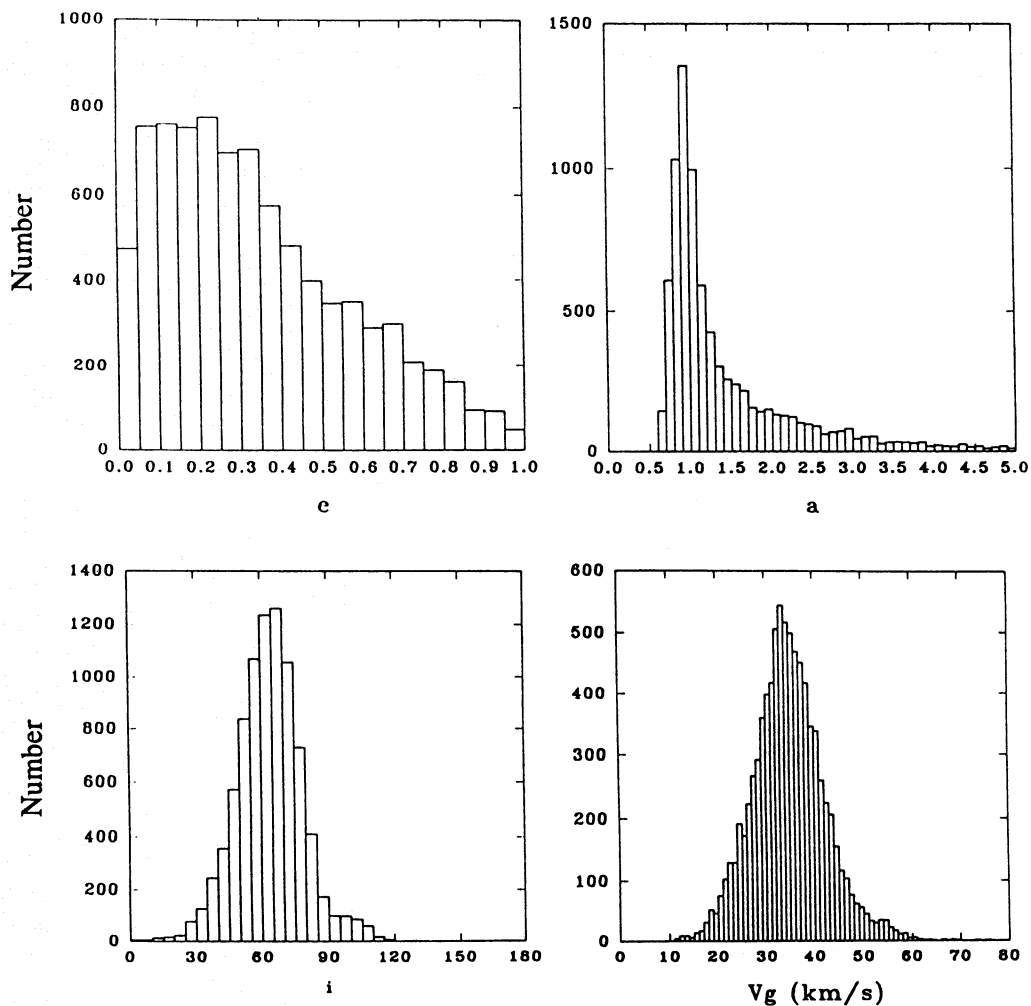


Figure 9. The orbital elements for the north toroidal source region. Details as in caption to Fig. 7.

suggested. Such highly inclined orbits are relatively stable. It is, however, difficult to envision the geometry that might lead to a single source producing radiant in the northern and southern hemispheres separated by some 120° . Alternatively, the possibility that $i=60^\circ$ is a particularly stable orbital inclination may lead to a selection effect favouring such particles. An examination of the distribution of NT particles throughout the year in the Harvard data revealed the source to be always present without showing large variations. Similarly, the ST source for which few data are available reflects essentially the same behaviour as its more-studied northern cousin.

ACKNOWLEDGMENTS

The authors thank B. A. Lindblad for making the data from the IAUMDC available to them, and David Hughes for his thoughtful comments and suggestions. This work was funded by a grant from the Natural Sciences and Engineering Research Council of Canada.

REFERENCES

Baggaley W. J., Steel D. I., Taylor A. D., 1992, in Harris A. W., Bowell E., eds, *Asteroids Comets and Meteors*. Lunar and Planetary Institute, Houston, Texas, p. 37

- Cook A. F., 1973, in Hemenway C. L., Millman P. M., Cook A. F., eds, *Evolutionary and Physical Properties of Meteoroids*. NASA SP-319, U.S. Government Printing Office, Washington, D.C., p. 183
- Davies J. G., 1957, *Adv. in Electronics and Electron Phys.*, 9, 95
- Davies J. G., Gill J. C., 1960, *MNRAS*, 121, 437
- Denning W. F., 1886, *MNRAS*, 47, 35
- Denning W. F., 1899, *Mem. R. Astron. Soc.*, 53, 203
- Hawkins G. S., 1956a, *AJ*, 61, 386
- Hawkins G. S., 1956b, *MNRAS*, 116, 92
- Hawkins G. S., Prentice J. P. M., *AJ*, 62, 234
- Hoffmeister C., 1948, *Meteorströme*, Verlag Werden und Werken Weimar, Leipzig
- Keay C. S. L., 1963, *MNRAS*, 25, 507
- Lindblad B. A., 1968, in Kresak L., Millman P. M., eds, *Physics and Dynamics of Meteors*. Reidel, Dordrecht, p. 50
- Lindblad B. A., 1987, *Publ. Astron. Inst. Czech.*, 67, 201
- Lindblad B. A., 1992, *Documentation of Meteor Data available at the IAUMDC*, preprint
- McCrosky R. C., Posen A., 1961, *Smithson. Contr. Astrophys.*, 4, 15
- McKinley D. W. R., 1961, *Meteor Science and Engineering*. McGraw-Hill, New York
- Meeks M. L., James J. C., 1959, *JATP*, 16, 228
- Murakami T., 1956, *PASJ*, 8, 87
- Schiaparelli G. V., 1866, *Sternschnuppen*, von der Nahmer, Stettin
- Sekanina Z., 1976, *Icarus*, 27, 265
- Stohl J., 1968, in Kresak L., Millman P. M., eds, *Physics and Dynamics of Meteors*. Reidel, Dordrecht, p. 298
- von Niessl G., 1878, *Astron. Nachr.*, 93, 209
- Weiss A. A., Smith J. W., 1960, *MNRAS*, 121, 5
- Weitzen J. A., 1986, *Radio Science*, 21, 1009